Bioprocessing and Biomass Technology

Journal homepage: https://bioprocessing.utm.my

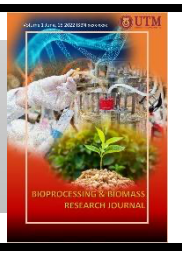

Research Article

Computational Analysis of Crosslinker Binding Affinity and Site Interactions with Fungal and Bacterial Laccases to Guide CLEA Development

Muhamad Faqih[a], Mohammad Nashriq Jailani[a], Rosli Md Illias[a], Nardiah Rizwana Jaafar[a*]

[a] *Department of Bioprocess and Polymer Engineering, Faculty of Chemical and Energy Engineering, Universiti Teknologi Malaysia, 81310 Skudai, Johor, Malaysia*

ARTICLE INFO

Article History:
Received 29 October 2025
Received in revised form 1 December 2025
Accepted 5 December 2025
Available online 30 December 2025

Keywords:
Laccase,
Molecular Docking,
Enzyme Immobilization

ABSTRACT

Efficient cross-linked enzyme aggregate (CLEA) formation requires not only strong interactions between enzymes and crosslinkers but also proper binding orientation to prevent active site obstruction. In this study, molecular docking was employed to investigate the interactions between fungal (*Trametes versicolor*) and bacterial (*Bacillus subtilis*) laccases and various crosslinkers, including glutaraldehyde, ethylene glycol, dialdehyde starch, pectin, and chitosan. Docking simulations revealed that chitosan exhibited the strongest binding affinity with both enzymes (-7.1 and -7.0 kcal/mol), primarily due to extensive hydrogen bonding and hydrophobic interactions. Binding site analysis further demonstrated that chitosan binds at sites distant from the active sites of the enzymes, which are 32.0 Å from the catalytic center within domain 2 of the bacterial laccase and 34.6 Å from the catalytic center within domain 3 of the fungal laccase, minimizing the risk of active site obstruction and preserving catalytic accessibility. In contrast, glutaraldehyde and ethylene glycol were found near the fungal laccase active site, potentially influencing substrate access. This study suggests that molecular docking can serve as a valuable preliminary approach to explore crosslinker–enzyme interactions and support the rational design of CLEAs before experimental validation.

INTRODUCTION

Laccases, belonging to the multicopper oxidase (MCO) enzyme family and classified as benzenediol oxygen reductases (EC 1.10.3.2), are enzymes characterized by their low substrate specificity and wide occurrence in nature. As their name implies, MCOs contain four copper ions organized into two distinct sites. The type 1 copper site receives an electron from the substrate and transfers it via a conserved His–Cys–His motif to the trinuclear center, which consists of one type 2 and two type 3 copper ions. This trinuclear center catalyzes the four-electron reduction of molecular oxygen (O_2) to water, using electrons derived from the substrate molecules (Arregui et al., 2019). These catalytic features enable laccases to participate in various mechanisms, for instance, monomer cross-linking, ring cleavage of aromatic complexes, and polymer degradation (Panwar et al., 2023). Owing to their broad substrate range, laccases can oxidize various phenolic and non-phenolic compounds, enabling their use in diverse industrial processes such as cotton bleaching, fruit juice clarification, wine stabilization, biosensor development, and bioremediation (Moreno et al., 2020). Additionally, laccases are found in higher plants, bacteria, fungi, and insects. However, fungi are the predominant producers, followed by bacteria (Debnath & Saha, 2020). Microbial laccases, particularly those from bacterial and fungal sources, are advantageous because they can be produced in large quantities using inexpensive substrates, thereby reducing production costs and making industrial application more feasible (Loi et al., 2021).

Despite the usefulness of enzymes, the full potential of enzymes for industrial applications remains underutilized.

*Corresponding Author
E-mail address: nardiah@utm.my*.
DOI address: 10.11113/bioprocessing.v4n2.81

The widespread application of enzymes remains constrained by their susceptibility to denaturation under severe operational conditions, including extreme pH, elevated temperatures, and exposure to solvents, surfactants, or metal ions. These limitations are further exacerbated by their relatively short storage stability and, most critically, the inherent difficulty in recovering and reusing the enzymes (Basso & Serban, 2019; Bié et al., 2022). Among these enzymes, laccase faces similar limitations. Although free laccase exhibits high catalytic activity, its practical application is limited by its inability to be separated and reused, leading to activity loss during continuous operation and an increase in overall production cost (Masjoudi et al., 2021). Moreover, free laccase often demonstrates poor stability when exposed to harsh operational conditions or during long-term storage (Wen et al., 2019). To overcome these limitations, enzyme immobilization has emerged as one of the most effective strategies. Among immobilization methods, carrier-free immobilization represents a promising approach for industrial applications, as it reduces production costs and enhances enzyme performance. In this method, enzymes are first precipitated and subsequently cross-linked using a suitable agent to form cross-linked enzyme aggregates (CLEAs). This approach is simple, economical, and efficient, since the main component of CLEAs is the enzyme itself (Chauhan et al., 2022).

However, developing efficient CLEAs requires compatibility between the enzyme and the chosen cross-linker. The formation of stable and efficient CLEAs largely relies on how amino acid residues interact with the crosslinker during the cross-linking step (Rodrigues et al., 2014). Cross-linkers typically contain reactive functional groups such as amine, thiol, or carboxyl, which must effectively interact with the corresponding amino acid residues on the enzyme surface. Because each enzyme has a unique amino acid composition and active site configuration, the same cross-linker can produce varying results depending on the enzyme. It is crucial that cross-linkers do not react with residues located in or near the active site, as this can result in enzyme deactivation (Sampaio et al., 2022). An oriented immobilization protocol is therefore highly desirable, as it ensures that the enzyme's active site remains accessible to substrates. Proper orientation during immobilization enhances catalytic efficiency and results in more uniform activity compared with conventional random immobilization methods (Robescu & Bavaro, 2025). Understanding the interactions between cross-linkers and enzymes during CLEA formation is thus essential for designing effective immobilization systems.

In recent years, molecular docking has become an important computational technique in the field of in-silico biomolecular research, particularly in drug discovery and enzyme design (*Sahoo et al., 2022*). This method allows prediction of binding affinity and identification of interaction sites in various complexes, including protein–ligand, protein–DNA, and protein–protein systems (Barati et al., 2024). By revealing the molecular interactions underlying binding mechanisms, molecular docking provides valuable insight into biochemical processes (Meng et al., 2011). Because screening cross-linkers experimentally can be time-consuming and labour-intensive, molecular docking can be a powerful tool to guide the selection of suitable cross-linkers for CLEA preparation (Jailani et al., 2022). Khan et al. (2019) successfully applied docking simulations to investigate the interaction between β-galactosidase and a polyaniline–chitosan–silver nanocomposite. Their results showed that the enzyme binds to the composite in a favourable orientation, and none of the immobilization interactions involve the enzyme's active site. As a result, the immobilized β-galactosidase retained 94% of its activity and exhibited a lower Km value compared to the free enzyme.

Therefore, this study aims to identify the most suitable cross-linker for the preparation of CLEAs from fungal and bacterial laccases using molecular docking analysis. Docking simulations were performed to evaluate the binding affinity and the specific interactions between cross-linkers and amino acid residues of the enzymes. Furthermore, the binding site of immobilization was analyzed to assess whether certain cross-linkers could cause substrate diffusion limitations. The findings demonstrated that chitosan was the most effective cross-linker for both fungal and bacterial laccases. Computational docking can therefore provide useful preliminary insights into crosslinker binding behaviours, guiding subsequent experimental strategies for efficient CLEA development.

MATERIALS AND METHOD

Materials

The three-dimensional (3D) structures of bacterial and fungal laccases were obtained from the Protein Data Bank (PDB) with accession codes 4YVN and 1KYA, respectively. The two-dimensional (2D) structures of several crosslinkers, namely chitosan, dialdehyde starch, ethylene glycol, glutaraldehyde, and pectin, were generated using ChemDraw Professional.

Cross-linker Preparation

The 3D structures of the cross-linkers were generated from their corresponding 2D structures using Avogadro (Hanwell et al., 2012). Hydrogen atoms were added by adjusting the system to pH 7, after which geometry optimization was carried out using the MMFF94 force field with 10,000 steps and the conjugate gradient algorithm. This optimization step was conducted to identify the most stable conformation of each cross-linker by adjusting bond lengths, bond angles, and dihedral angles to minimize potential energy, thereby ensuring structural accuracy for subsequent molecular docking analyses (Roy et al., 2015).

Laccase–Cross-linker Docking Simulation

Molecular docking simulations between laccases and the cross-linkers were carried out using AutoDock Vina 1.27 (Eberhardt et al., 2021). The enzymes were prepared using Dock Prep prior to docking, including completing missing side chain, adding hydrogen, and adding charges (Maier et al., 2015; Shapovalov & Dunbrack, 2011). Docking preparation was conducted following the procedure described by Yip et al. (2023), with some adjustments. The grid box dimensions were set to 70 × 70 × 70 Å for both enzymes to ensure complete coverage of the enzyme structures. The exhaustiveness value was set to 8, and the maximum energy difference was 3 kcal/mol. Default docking parameters were applied, except that the option ignoring all non-standard residues was set to *false*.

Structural Analysis

Docking output files in .pdbqt format were converted to .pdb format for visualization. The resulting .pdb files of each

docked complex were merged with the corresponding enzyme structure using PyMOL to generate a single complex file containing both the enzyme and its bound cross-linker. The molecular interactions between laccase and each cross-linker were analyzed using LigPlot+ (Laskowski & Swindells, 2011) to identify hydrogen bonds and hydrophobic interactions.

RESULTS AND DISCUSSION

Docking Analysis of Bacterial and Fungal Laccase with Different Types of Crosslinkers

Molecular docking simulations were performed to evaluate the binding interactions between bacterial and fungal laccases and several cross-linkers, including glutaraldehyde, ethylene glycol, dialdehyde-starch, pectin, and chitosan. Binding affinities, hydrogen bonding, and hydrophobic interactions were analysed to understand the interactions between the residues of the enzymes and the crosslinkers. **Table 1** summarizes the binding energies and the key interaction types for all enzymes and crosslinkers.

Table 1 Summary of binding energies and key interaction types for all enzyme–crosslinker systems.

Crosslinker	Enzyme	Binding Energy (kcal/mol)	Hydrogen Bonds	Hydrophobic Interactions
Glutaraldehyde	Fungal	-3.7	3	3
	Bacterial	-4.1	1	4
Ethylene Glycol	Fungal	-3.4	6	2
	Bacterial	-3.5	5	3
Dialdehyde Starch	Fungal	-5.9	8	6
	Bacterial	-6.2	10	7
Pectin	Fungal	-6.6	4	9
	Bacterial	-7.1	10	11
Chitosan	Fungal	-7.0	7	6
	Bacterial	-7.1	7	8

Glutaraldehyde

The binding affinities of bacterial and fungal laccases with glutaraldehyde were -4.1 and -3.7 kcal/mol, respectively. In AutoDock Vina, the binding energy score is obtained from the sum of several individual terms, including a combined attractive term that accounts for van der Waals interactions, hydrogen bonding, and hydrophobic effects, as well as a repulsive term and a conformational entropy penalty (Eberhardt et al., 2021). A lower binding energy score indicates stronger protein–ligand binding affinity (Fan et al., 2019). **Figure 1** shows the 2D interactions of bacterial laccase and fungal laccase with glutaraldehyde. The slight difference in binding energy primarily results from variations in hydrogen bonding interactions. In the fungal laccase–glutaraldehyde complex, both aldehyde oxygen atoms participated in hydrogen bonding, forming a more extensive interaction network. Specifically, the O_2 atom of glutaraldehyde established hydrogen bonds with Arg423 (3.000 Å) and Gln242 (3.056 Å), while the O_1 atom interacted with Glu302 (2.916 Å). In contrast, the bacterial laccase–glutaraldehyde complex exhibited only one hydrogen bond, in which the O_1 atom of glutaraldehyde was linked to His89 (3.023 Å). In contrast, the bacterial laccase–glutaraldehyde complex exhibited only one hydrogen bond, in which the O_1 atom of glutaraldehyde was linked to His89 (3.023 Å). These findings indicate that fungal laccase provides a more favourable polar environment for glutaraldehyde binding compared to bacterial laccase.

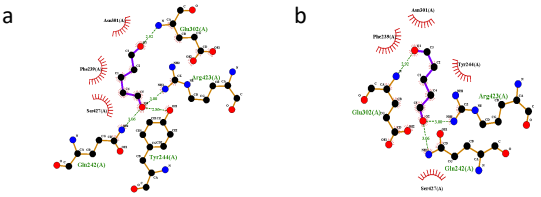

Figure 1 2D interaction profiles of (a) fungal laccase and (b) bacterial laccase with glutaraldehyde. Green dashed lines indicate hydrogen bond interactions, while red lines represent hydrophobic interactions.

Hydrophobic interactions between both enzymes and glutaraldehyde were also evaluated. These interactions provide important insights into the stability of the complex, as nonpolar contacts often drive the enzyme to undergo conformational adjustments to better accommodate the ligand, a phenomenon known as induced fit (Davis & Teague, 1999). In terms of hydrophobic interactions, bacterial laccase demonstrated more extensive non-polar contacts with glutaraldehyde than fungal laccase. The hydrophobic residues contributing to bacterial laccase binding included Phe239, Asn301, Ser427, and Tyr244, forming a compact hydrophobic microenvironment. Conversely, the fungal laccase–glutaraldehyde complex showed fewer hydrophobic interactions, primarily involving Asn301, Phe239, and Ser427.

Ethylene Glycol

The docking simulations revealed comparable binding affinities of bacterial and fungal laccases toward ethylene glycol, with values of -3.5 and -3.4 kcal/mol, respectively. **Figure 2** illustrates the 2D interaction profiles of both enzyme–ethylene glycol complexes. The close similarity in binding energies can be attributed to the comparable number of residues involved in the interactions. In the fungal laccase–ethylene glycol complex, the O_1 atom formed hydrogen bonds with Arg423 (3.098 Å), Tyr244 (2.995 Å), and Gln242 (2.862 Å, 3.075 Å), while the O_2 atom was linked to Ser427 (3.165 Å) and Gln242 (2.850 Å). Similarly, in the bacterial laccase–ethylene glycol complex, the O_1 atom established hydrogen bonds with Ser349 (2.891 Å), Glu348 (2.923 Å), and Arg248 (3.016 Å, 2.966 Å), whereas the O_2 atom interacted with Ser186 (2.960 Å). These findings suggest that both enzymes exhibit comparable polar binding characteristics with ethylene glycol.

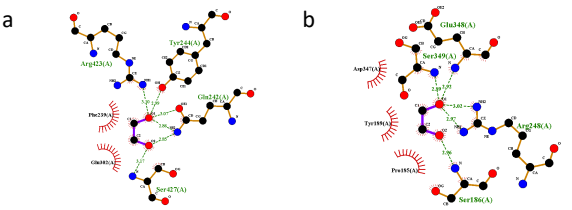

Figure 2 2D interaction profiles of (a) fungal laccase and (b) bacterial laccase with ethylene glycol. Green dashed lines indicate hydrogen bond interactions, while red lines represent hydrophobic interactions.

In addition to hydrogen bonding, hydrophobic interactions contributed to the stabilization of both complexes. For fungal laccase, hydrophobic contacts were observed with residues Glu302 and Phe239. Meanwhile, bacterial laccase exhibited hydrophobic interactions with Asp347, Tyr189, and Pro185. The similar number and

distribution of hydrophobic residues further support the nearly identical binding energies of ethylene glycol toward both bacterial and fungal laccases, indicating that both enzymes share a comparable affinity and binding mode for this diol crosslinker.

Dialdehyde-starch

The docking analysis revealed binding affinities of -6.2 and -5.9 kcal/mol for bacterial and fungal laccases, respectively, indicating a comparable interaction strength with dialdehyde starch. **Figure 3** shows the 2D interactions of bacterial laccase and fungal laccase with dialdehyde starch. Similar to the interaction pattern observed with glutaraldehyde, the difference in binding energy is primarily influenced by the number of hydrogen bonds and the extent of oxygen atom interactions with the enzyme residues. In the fungal laccase–dialdehyde starch complex, hydrogen bonds were established with Arg442 (2.845 Å, 3.173 Å, 3.164 Å), His402 (3.137 Å), Asn227 (3.000 Å, 3.014 Å, 3.205 Å), Ser225 (2.860 Å), and Ala103 (3.242 Å). Meanwhile, in the bacterial laccase–dialdehyde starch complex, hydrogen bonding interactions occurred with Arg248 (2.816 Å, 3.138 Å, 3.137 Å, 3.293 Å), Ser186 (3.048 Å, 3.147 Å), Ser349 (3.149 Å), Glu348 (3.126 Å), Leu184 (2.866 Å), Glu179 (3.131 Å), Asp176 (3.228 Å), and Pro185 (2.869 Å). These results indicate that both enzymes form extensive polar interactions with dialdehyde starch, though bacterial laccase engages a greater number of amino acid residues.

a b

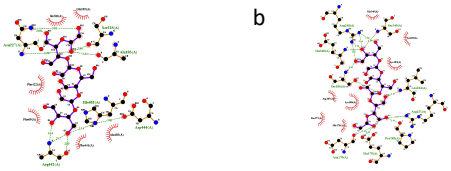

Figure 3 2D interaction profiles of (a) fungal laccase and (b) bacterial laccase with dialdehyde starch. Green dashed lines indicate hydrogen bond interactions, while red lines represent hydrophobic interactions.

The slightly stronger binding affinity of bacterial laccase compared to fungal laccase can also be attributed to its higher number of hydrophobic contacts, with 7 residues compared to 6. In fungal laccase, hydrophobic interactions were primarily formed with Arg442, Ile226, Gln102, Phe441, Phe69, and Ala403. In contrast, bacterial laccase exhibited hydrophobic interactions involving Gln345, Tyr189, Asp187, Pro177, Lys183, Lys180, and His175.

Pectin

The binding affinities of bacterial and fungal laccases with pectin were -7.1 and -6.6 kcal/mol, respectively. **Figure 4** shows the 2D interaction profiles of both laccase–pectin complexes. Hydrogen bonding primarily occurred through the hydroxyl groups of the pectin backbone. The notable difference in binding energies can be attributed to the number of hydrogen bonds formed. In the fungal laccase–pectin complex, hydrogen bonds were established with Arg442 (2.903 Å), Ala403 (2.928 Å), and Asn227 (3.039 Å, 2.990 Å). In contrast, the bacterial laccase–pectin complex exhibited a larger number of hydrogen bonds, interacting with Thr418 (3.013 Å, 2.991 Å, 3.076 Å), Thr262 (3.243 Å, 3.156 Å), Gln468 (3.099 Å), Gly321 (3.097 Å, 2.845 Å), His419 (3.049 Å), Thr415 (2.934 Å), and Gly417 (2.992 Å).

a b

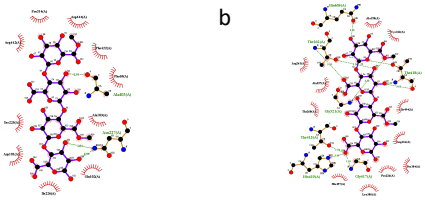

Figure 4 2D interaction profiles of (a) fungal laccase and (b) bacterial laccase with pectin. Green dashed lines indicate hydrogen bond interactions, while red lines represent hydrophobic interactions.

Although the overall hydrogen bonding pattern, including the number, type, and location of interactions, is comparable to that observed with dialdehyde starch, hydrophobic interactions appear to play a more decisive role in stabilizing the laccase–pectin complexes. In the fungal laccase complex, these interactions involved Asp444, Phe422, Pro314, Ile226, Ser225, Ala103, Gln102, Asp101, and Phe69. Meanwhile, in the bacterial laccase complex, hydrophobic contacts were formed with His497, Ile494, Leu386, Pro384, Cys322, Arg416, Ala320, Arg261, Thr260, Ala227, and Pro226. The greater number of hydrophobic interactions in the bacterial laccase complex likely also contributes to its stronger binding affinity compared to the fungal enzyme.

Chitosan

The binding affinities of bacterial and fungal laccases with chitosan were -7.1 and -7.0 kcal/mol, respectively, representing the strongest interactions among all the crosslinkers investigated. This high affinity can be attributed to the presence of amino groups in chitosan, which facilitate extensive hydrogen bonding with both enzymes. The slight difference in binding energies is consistent with the similar number of hydrogen bonds formed in both complexes. **Figure 5** shows the 2D interactions of chitosan with both enzymes. In the bacterial laccase–chitosan complex, hydrogen bonds were established with Ser186 (3.049 Å, 2.854 Å), Arg248 (2.913 Å), Lys346 (3.234 Å), Lys183 (3.265 Å), and Leu184 (2.944 Å, 2.960 Å, 2.924 Å). Conversely, in the fungal laccase–chitosan complex, hydrogen bonding interactions were observed with Asp444 (2.972 Å, 3.215 Å), His402 (3.177 Å, 2.801 Å), Gly401 (3.066 Å), Ser225 (2.915 Å), and Ala103 (2.849 Å, 3.260 Å, 3.258 Å).

a b

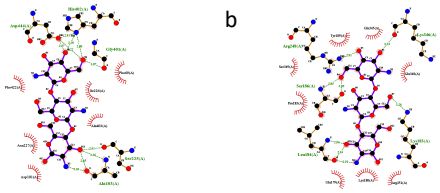

Figure 5 2D interaction profiles of (a) fungal laccase and (b) bacterial laccase with chitosan. Green dashed lines indicate hydrogen bond interactions, while red lines represent hydrophobic interactions.

Hydrophobic interactions further contributed to the stability of the complexes. In the fungal laccase–chitosan complex, these interactions involved Phe422, Ala403, Asp101, Phe69, Asn227, and Ile226. Meanwhile, the bacterial laccase complex exhibited hydrophobic contacts with Ser349, Glu179, Gln345, Arg251, Glu348, Tyr189, Pro185, and Lys180. The greater number of amino acid residues involved in hydrophobic interactions with bacterial

laccase may explain its slightly stronger binding affinity compared to the fungal enzyme.

Binding Site Analysis of Crosslinkers

In the formation of CLEAs, not only the interactions between the enzyme and crosslinker but also the binding location are important. This is because binding near or within the active site can obstruct substrate access and potentially reduce enzyme activity after immobilization (Yu et al., 2022). The structural orientation of the interactions between the enzymes and the crosslinkers is summarized in **Table 2**.

Table 2 Structural orientation of crosslinker binding domains and their distances from the catalytic centers of bacterial and fungal laccases.

Crosslinker	Enzyme	Binding Domain	Distance from Catalytic Center (Å)
Glutaraldehyde	Bacterial	Domain 2	38.6
	Fungal	Domain 2	19.5
Ethylene Glycol	Bacterial	Domain 2	36.9
	Fungal	Domain 2	18.7
Dialdehyde Starch	Bacterial	Domain 2	29.9
	Fungal	Domain 3	33.2
Chitosan	Bacterial	Domain 2	32.0
	Fungal	Domain 3	34.6
Pectin	Bacterial	Domain 2	28.4
	Fungal	Domain 3	36.0

Laccases from *Trametes versicolor* and *Bacillus subtilis* contain three types of copper ions based on their magnetic and spectroscopic properties: type 1 (T1), type 2 (T2), and a binuclear type 3 (T3) copper center. These enzymes are composed of three structural domains. Domain 2 plays a crucial role in maintaining the overall enzyme architecture by connecting and properly positioning domains 1 and 3 in the three-domain laccase structure. The mononuclear T1 copper site, which serves as the primary active site for substrate oxidation, is located in domain 3, while the trinuclear T2/T3 copper cluster is formed at the interface between domains 1 and 3 (Hakulinen & Rouvinen, 2015).

Figure 6 presents the 3D structure of the bacterial laccase and crosslinkers. As shown in **Figure 6**, the active site of the bacterial laccase is highlighted as a purple surface, while the regions where the crosslinkers interact are shown in red. In all five complexes, the red interaction patches are located far from the purple active site region, confirming that none of the crosslinkers bind near the catalytic center. Instead, all interactions occur at distant regions, primarily in domain 2 of the enzyme. The measured distances between the binding sites and the catalytic center are 38.6 Å for glutaraldehyde, 36.9 Å for ethylene glycol, 32.0 Å for chitosan, 29.9 Å for dialdehyde starch, and 28.4 Å for pectin. This suggests that crosslinker binding is unlikely to directly interfere with the catalytic function of the enzyme, allowing the active site to remain accessible for substrate oxidation. These findings are consistent with molecular docking results reported by Ali et al. (2018), who demonstrated that a polypyrrole–cellulose–graphene oxide nanocomposite bound guaiacol peroxidase at a site located far from its catalytic center. The distal binding predicted in that study aligned with experimental observations showing a slight decrease in Km for the immobilized enzyme, confirming that the active site remained unobstructed and that substrate affinity was improved.

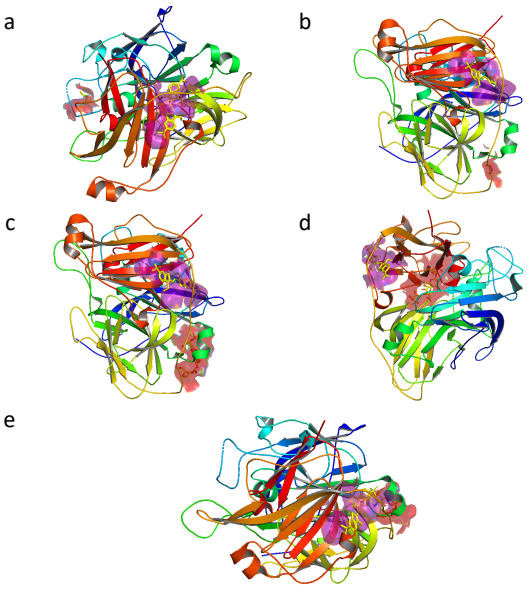

Figure 6 3D interaction structures of the bacterial laccase with (a) glutaraldehyde, (b) ethylene glycol, (c) dialdehyde starch, (d) pectin, and (e) chitosan. The active site is shown as a purple surface, while the red surface represents the interaction regions with the crosslinkers.

Figure 7 shows the 3D structure of the fungal laccase with bound crosslinkers. Glutaraldehyde (19.5 Å, domain 2) and ethylene glycol (18.7 Å, domain 2) are located near the active site region, suggesting a potential influence on catalytic activity or substrate accessibility. In contrast, the other crosslinkers bind on the opposite side of the enzyme, primarily within domain 3, and are positioned away from the active site. The measured distances from the catalytic center for these crosslinkers are 33.2 Å for dialdehyde starch, 34.6 Å for chitosan, and 36.0 Å for pectin. This makes them less likely to directly influence catalytic activity. This observation aligns with the findings of Khongkomolsakul et al. (2025) who reported that, in the phytase–polysaccharide complexes, sulfated polysaccharides (iota (IC), lambda (LC), and kappa (KC) carrageenan) were bound directly within the active-site pocket, whereas carboxylated polysaccharides (low-methoxyl pectin (LMP) and sodium alginate (SA)) occupied positions away from the active site. As a result, the lower activity recovery observed for IC and LC was attributed to their proximity to the catalytic region, while polysaccharides binding at distal regions did not hinder enzymatic function.

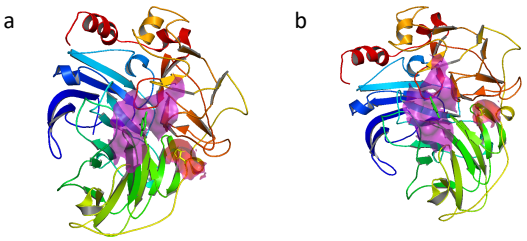

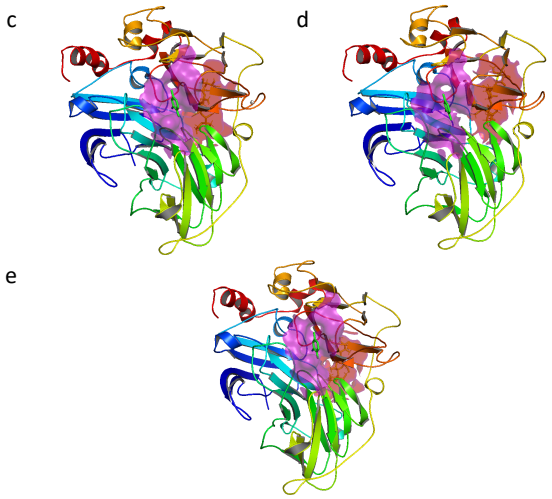

Figure 7 3D interaction structures of the fungal laccase with (a) glutaraldehyde, (b) ethylene glycol, (c) dialdehyde starch, (d) pectin, and (e) chitosan. The active site is shown as a purple surface, while the red surface represents the interaction regions with the crosslinkers.

CONCLUSION

In conclusion**,** this study aimed to elucidate the interactions between bacterial and fungal laccases and various crosslinkers through molecular docking analysis prior to CLEA development. The results showed that chitosan exhibited the strongest binding affinity with both enzymes, with binding energies of -7.0 and -7.1 kcal/mol, respectively. Furthermore, binding site analysis revealed that chitosan was positioned far from the active sites of both enzymes, thereby minimizing potential disruption to catalytic activity and allowing proper enzyme orientation during immobilization. Despite these promising findings, it should be noted that docking simulations provide only static predictions and cannot fully account for crosslinking efficiency, enzyme flexibility, or structural behaviour under reaction conditions. To better reflect how these interactions behave under dynamic conditions, future studies should incorporate molecular dynamics simulations and subsequently verify the findings experimentally through CLEA synthesis, activity recovery tests, stability assessments, and reusability evaluations. This combined approach will be crucial for confirming the practical performance of the selected crosslinkers.

Acknowledgement

This work is financially supported by Ministry of Higher Education under Fundamental Research Grant Scheme (FRGS/1/2022/TK08/UTM/02/16) and Universiti Teknologi Malaysia under UTM Fundamental Research (UTMFR) grant (PY/2022/01593).

Conflicts of Interest

The author declares that there is no conflict of interest regarding the publication of this paper.

References

Ali, M., Husain, Q., Sultana, S., & Ahmad, M. (2018). Immobilization of peroxidase on polypyrrole-cellulose-graphene oxide nanocomposite via non-covalent interactions for the degradation of Reactive Blue 4 dye. *Chemosphere*, 202, 198–207.

Arregui, L., Ayala, M., Gómez-Gil, X., Gutiérrez-Soto, G., Hernández-Luna, C. E., Herrera De Los Santos, M., Levin, L., Rojo-Domínguez, A., Romero-Martínez, D., & Saparrat, M. C. N. (2019). Laccases: structure, function, and potential application in water bioremediation. *Microbial Cell Factories*, 18, 1–33.

Barati, F., Hosseini, F., Vafaee, R., Sabouri, Z., Ghadam, P., Arab, S. S., ... & Piroozmand, F. (2024). In silico approaches to investigate enzyme immobilization: a comprehensive systematic review. *Physical Chemistry Chemical Physics*, *26*(7), 5744-5761.

Basso, A., & Serban, S. (2019). Industrial applications of immobilized enzymes—A review. *Molecular Catalysis*, 479, 110607.

Bié, J., Sepodes, B., Fernandes, P. C. B., & Ribeiro, M. H. L. (2022). Enzyme immobilization and co-immobilization: main framework, advances and some applications. *Processes*, 10(3), 494.

Chauhan, V., Kaushal, D., Dhiman, V. K., Kanwar, S. S., Singh, D., Dhiman, V. K., & Pandey, H. (2022). An insight in developing carrier-free immobilized enzymes. *Frontiers in Bioengineering and Biotechnology*, 10, 794411.

Davis, A. M., & Teague, S. J. (1999). Hydrogen bonding, hydrophobic interactions, and failure of the rigid receptor hypothesis. *Angewandte Chemie International Edition*, 38(6), 736–749.

Debnath, R., & Saha, T. (2020). An insight into the production strategies and applications of the ligninolytic enzyme laccase from bacteria and fungi. *Biocatalysis and Agricultural Biotechnology*, 26, 101645. https://doi.org/https://doi.org/10.1016/j.bcab.2020.101645

Eberhardt, J., Santos-Martins, D., Tillack, A. F., & Forli, S. (2021). AutoDock Vina 1.2. 0: New docking methods, expanded force field, and python bindings. *Journal of Chemical Information and Modeling*, 61(8), 3891–3898.

Fan, J., Fu, A., & Zhang, L. (2019). Progress in molecular docking. *Quantitative Biology*, 7(2), 83–89.

Hakulinen, N., & Rouvinen, J. (2015). Three-dimensional structures of laccases. *Cellular and Molecular Life Sciences*, 72(5), 857–868.

Hanwell, M. D., Curtis, D. E., Lonie, D. C., Vandermeersch, T., Zurek, E., & Hutchison, G. R. (2012). Avogadro: an advanced semantic chemical editor, visualization, and analysis platform. *Journal of Cheminformatics*, 4, 1–17.

Jailani, N., Jaafar, N. R., Suhaimi, S., Mackeen, M. M., Bakar, F. D. A., & Illias, R. M. (2022). Cross-linked cyclodextrin glucanotransferase aggregates from *Bacillus lehensis* G1 for cyclodextrin production: Molecular modeling, developmental, physicochemical, kinetic and thermodynamic properties. *International Journal of Biological Macromolecules*, 213, 516–533.

Khan, M., Husain, Q., & Ahmad, N. (2019). Elucidating the binding efficacy of β-galactosidase on polyaniline–chitosan nanocomposite and polyaniline–chitosan–silver nanocomposite: activity and molecular docking insights. *Journal of Chemical Technology & Biotechnology*, 94(3), 837–849.

Khongkomolsakul, W., Yang, E., Dadmohammadi, Y., Dong, H., Lin, T., Huang, Y., & Abbaspourrad, A. (2025). Enzyme immobilization with plant-based

polysaccharides through complex coacervation. *LWT*, 219, 117537.

Laskowski, R. A., & Swindells, M. B. (2011). LigPlot+: multiple ligand–protein interaction diagrams for drug discovery. *ACS Publications*, 2788-2786.

Loi, M., Glazunova, O., Fedorova, T., Logrieco, A. F., & Mulè, G. (2021). Fungal laccases: The forefront of enzymes for sustainability. *Journal of Fungi*, 7(12), 1048.

Maier, J. A., Martinez, C., Kasavajhala, K., Wickstrom, L., Hauser, K. E., & Simmerling, C. (2015). ff14SB: improving the accuracy of protein side chain and backbone parameters from ff99SB. *Journal of Chemical Theory and Computation*, 11(8), 3696–3713.

Masjoudi, M., Golgoli, M., Nejad, Z. G., Sadeghzadeh, S., & Borghei, S. M. (2021). Pharmaceuticals removal by immobilized laccase on polyvinylidene fluoride nanocomposite with multi-walled carbon nanotubes. *Chemosphere*, 263, 128043.

Meng, X.-Y., Zhang, H.-X., Mezei, M., & Cui, M. (2011). Molecular docking: a powerful approach for structure-based drug discovery. *Current Computer-Aided Drug Design*, 7(2), 146–157.

Moreno, A. D., Ibarra, D., Eugenio, M. E., & Tomás-Pejó, E. (2020). Laccases as versatile enzymes: from industrial uses to novel applications. *Journal of Chemical Technology & Biotechnology*, 95(3), 481–494.

Panwar, V., Lzaod, S., & Dutta, T. (2023). Thermostable bacterial laccase: catalytic properties and its application in biotransformation of emerging pollutants. *ACS Omega*, 8(38), 34710–34719.

Robescu, M. S., & Bavaro, T. (2025). A comprehensive guide to enzyme immobilization: All you need to know. *Molecules*, 30(4), 939.

Rodrigues, R. C., Barbosa, O., Ortiz, C., Berenguer-Murcia, Á., Torres, R., & Fernandez-Lafuente, R. (2014). Amination of enzymes to improve biocatalyst performance: Coupling genetic modification and physicochemical tools. *RSC Advances*, 4(72), 38350–38374.

Roy, K., Kar, S., & Das, R. N. (2015). Chapter 5 - Computational Chemistry. In K. Roy, S. Kar, & R. N. Das (Eds.), Understanding the Basics of QSAR for Applications in Pharmaceutical Sciences and Risk Assessment (pp. 151–189). *Academic Press*. https://doi.org/https://doi.org/10.1016/B978-0-12-801505-6.00005-3

Sahoo, R. N., Pattanaik, S., Pattnaik, G., Mallick, S., & Mohapatra, R. (2022). Review on the use of Molecular Docking as the First Line Tool in Drug Discovery and Development. *Indian Journal of Pharmaceutical Sciences*, 84(5).

Sampaio, C. S., Angelotti, J. A. F., Fernandez-Lafuente, R., & Hirata, D. B. (2022). Lipase immobilization via cross-linked enzyme aggregates: Problems and prospects - A review. *International Journal of Biological Macromolecules*, 215, 434–449. https://doi.org/https://doi.org/10.1016/j.ijbiomac.2022.06.139

Shapovalov, M. V, & Dunbrack, R. L. (2011). A smoothed backbone-dependent rotamer library for proteins derived from adaptive kernel density estimates and regressions. *Structure*, 19(6), 844–858.

Wen, X., Zeng, Z., Du, C., Huang, D., Zeng, G., Xiao, R., Lai, C., Xu, P., Zhang, C., & Wan, J. (2019). Immobilized laccase on bentonite-derived mesoporous materials for removal of tetracycline. *Chemosphere*, 222, 865–871.

Yip, Y. S., Manas, N. H. A., Jaafar, N. R., Rahman, R. A., Puspaningsih, N. N. T., & Illias, R. M. (2023). Combined cross-linked enzyme aggregates of cyclodextrin glucanotransferase and maltogenic amylase from *Bacillus lehensis* G1 for maltooligosaccharides synthesis. *International Journal of Biological Macromolecules*, 242, 124675.

Yu, D., Wang, N., Gong, Y., Wu, Z., Wang, W., Wang, L., Wu, F., & Jiang, L. (2022). Screening of active sites and study on immobilization of *Bacillus cereus* phospholipase C. *LWT*, 159, 113245. https://doi.org/https://doi.org/10.1016/j.lwt.2022.113245